Asymmetric 2+1 pass stereo matching algorithm for real images

Chi Chu
National Chiao Tung University
Department of Computer Science
Hsinchu, Taiwan 300

Chin-Chen Chang
National United University
Department of Computer Science and Information Engineering
Miaoli, Taiwan 36003
E-mail: ccchang@nuu.edu.tw

Abstract. An asymmetric 2+1 pass stereo matching algorithm is proposed for generating a depth map from the input of two real stereo images. In the first pass, the Canny edge detector is used to acquire edge images from the inputs. Component images are then generated from the edge images. The edges of each component in the left component image are cut to obtain asymmetric left and right component images. The concept of a disparity-space image (DSI) by components is introduced and dynamic programming (DP) techniques are applied to match the asymmetric left and right component images. In the second pass, the previous DSI is modified, applying the DP methods to acquire the matched pixel pairs of the matched component pairs, and to generate ground control pairs (GCPs). In the final pass, these GCPs are incorporated into the DP algorithms to determine the optimal path and acquire the depth image. The results show that the proposed approach produces reliable and efficient matching and preserves the shapes of objects effectively for real stereo images. The proposed algorithm makes contours clearer than other conventional methods for real stereo images. © *2006 Society of Photo-Optical Instrumentation Engineers.* [DOI: 10.1117/1.2205182]

Subject terms: Three-dimensional computer vision; image-based rendering; shape from stereo; stereo matching.

Paper 050526R received Jun. 30, 2005; revised manuscript received Oct. 11, 2005; accepted for publication Oct. 17, 2005; published online May 19, 2006.

1 Introduction

Stereo matching is one of the most important aspects of computer vision. Recently, stereo matching has been intensively studied.[1–21] A typical stereo matching problem is calculating a depth map from a stereo pair. Dense output, for use in applications such as view synthesis, image-based rendering, and so on is an essential requirement.

Scharstein and Szeliski[17] compiled a good taxonomy of stereo matching algorithms. Although previous studies have provided many techniques for stereo matching, there are still numerous problems that have not yet been explored, especially for real stereo images. Therefore, in this paper, an asymmetric 2+1 pass stereo matching algorithm is presented to acquire a depth map from two real stereo images. Previous algorithms used ground control pairs[1] (GCPs), which are the trusted matched pixel pairs between stereo images, to guide the process of dynamic programming (DP) techniques. A new algorithm to generate these GCPs is presented here. Using these GCPs, the accuracy of the generated depth image is greatly improved. The results show that the proposed algorithm produces reliable and efficient matching and effectively preserves the shapes of objects. This approach also makes contours clearer than other traditional methods.

Figure 1 shows the diagram of the proposed algorithm. First, edge images from the inputs are obtained by using the Canny edge detector.[22] A component is a set of connected pixels. The connection between two pixels p_s and p_e is defined as if they are neighbors or there is a path p_s (p_1), $p_2, \ldots, p_i, p_{i+1}, \ldots, p_{n-1}, p_e$ (p_n) in which each two adjacent pixels p_i and p_{i+1} are neighbors. A component image contains several components. Then, we use the edge images to generate component images. Third, we cut the edges in the left component image to obtain asymmetric left and right component images. Fourth, the concept of a disparity-space image[1,6,11,20] (DSI) by components is introduced, and the DP techniques are applied to match the asymmetric left and right component images. After that, the previous DSI would be modified, applying the DP methods to acquire the matched pixel pairs of the matched component pairs, and to generate GCPs. Finally, these GCPs are incorporated into the DP algorithms to determine the optimal path and acquire the depth image.

The rest of this paper is organized as follows. Section 2 briefly discusses related works. Section 3 presents the proposed algorithm. Section 4 shows results. Analysis and discussion are given in Sec. 5 and conclusions are presented in Sec. 6.

2 Related Works

Stereo algorithms generally perform subsets of the following four steps[17]: matching cost computation (step 1), cost aggregation (step 2), disparity computation/optimization (step 3), and disparity refinement (step 4). Stereo matching algorithms can be roughly divided into local approaches and global methods according to the steps performed. One class of global optimization algorithms are those based on the DP algorithms. This approach computes the minimum cost path in DSI.

Ohta and Kanade[15] proposed a stereo matching algo-

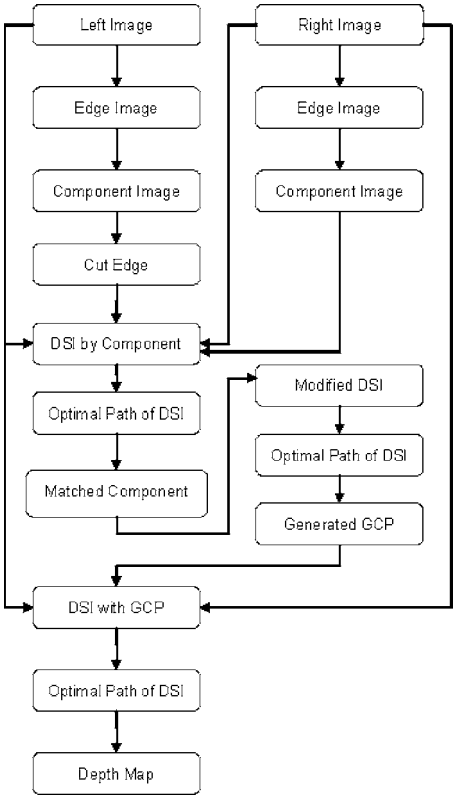

Fig. 1 Diagram of the proposed algorithm.

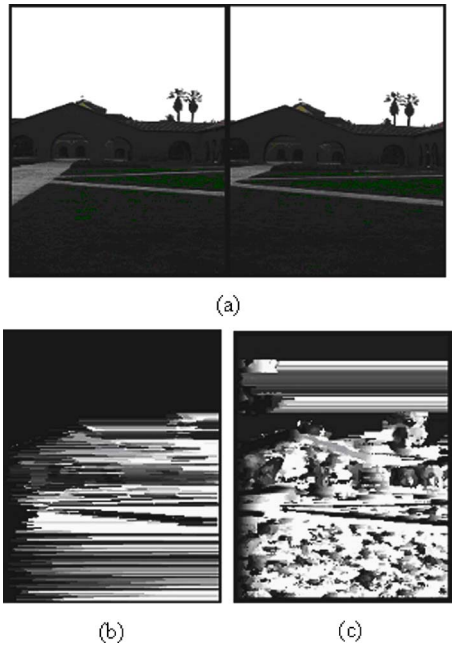

Fig. 2 (a) Real stereo input pair "Church," (b) a depth map generated by a global method with parameters set[17,21] as DPm1o20s0020, and (c) a depth map generated by a local approach with parameters set[17,21] as SAD09; the maximum disparity was set at 60.

rithm using the DP technique. Their approach computes an optimal solution in a 3-D search space. However, this approach yields only a sparse representation in terms of edges. Cox et al.[3] presented a maximum likelihood algorithm to overcome occlusion problems. This approach, however, requires more steps to iteratively compel smoothness constraints between epipolar lines. Bobick and Intille's approach[1] attempts to solve the stereo matching problem by using GCPs, since sensitivity to the occlusion cost can then be illuminated. There is, however, the problem with order constraint violations. Zitnick and Kanade[20] presented an algorithm for stereo matching and occlusion detection; they used global constraints to find a dense depth map. However, two assumptions, uniqueness and continuity, are necessary to produce disparity maps. Gong and Yang[6] proposed an approach for solving stereo matching problems by introducing the strong and weak consistency constraints; however, the computation cost of matching is high. Torr and Criminisi[19] improved on the dynamic programming approach for dense stereo. They introduced pivoting to modify the cost function of the DP techniques. But, it requires a unified dynamic programming/statistical framework.

When dealing with large-disparity stereo images, the generated depth image usually has incorrect depth estimations in some regions. The global methods work better for such stereo images than do the local methods. However, after analyzing results generated by the programs of Scharstein and Szeliski,[17,21] most of these global algorithms are not reliable for real stereo images. Due to the effect of global optimization, regions of different disparities are not clearly separated in the generated depth map. Figure 2(a) shows a real stereo input pair "Church," Fig. 2(b) shows a depth map generated using a global method with parameters set as DPm1o20s0020,[17,21] and Fig. 2(c) shows a depth map generated using a local approach with parameters[17,21] set as SAD09. Also, for Fig. 2, the maximum disparity was set at 60.

Therefore, this paper presents an asymmetric 2+1 pass stereo matching algorithm to acquire a depth map from two real stereo images. The most important data structure used in the proposed algorithm is DSI; it is assumed that a pair of rectified images is given as input.[17] Thus, in DSI, pixels in the left image shift horizontally to the right image. The DSI of row r is a 2-D array where the value of element DSI$[i][j]$ represents the matching value of pixel p at coordinates (r,j) in the left image and pixel q at coordinates $(r,j-i)$ in the right image. In practice, the value of similarity can be the absolute intensity difference, the correlation value of two pixels, and so on. The DSI illustrates all possible matching combinations of pixels in both the left and right image rows. To determine a correct combination, an optimal path on the DSI must be found that can be done with the DP method. A single pixel in the optimal path in the DSI has only three directions: horizontally right, which indicates a matching; diagonally down, which means occlusion in the left image; and vertically up, which is occlusion in the right image.[1] The optimal path can be found with these three restricted directions using the DP approach. When the optimal path is found, the disparities of pixels in one row are known, and then the depths can be determined.

3 Proposed Algorithm

An asymmetric 2+1 pass stereo matching algorithm called A21PASM is presented here to generate the depth map from the two given real stereo images.

The input to algorithm A21PASM is two real stereo images, the output is the depth map, and the steps of the proposed algorithm are as follows:

1. Compute edge images from the inputs by applying the Canny edge detector.
2. Generate component images from the edge images.
3. Obtain asymmetric left and right component images by using procedure ComponentCut to cut the edges of each component in the left component image.
4. Match the components between the asymmetric left and right component images by introducing the concept of DSI by the components and applying DP techniques to find the optimal path of the DSI.
5. Modify the previous DSI, use the DP approaches to acquire the matched pixel pairs between the matched component pairs, and generate the GCPs.
6. Incorporate the GCPs into the DSI, use the DP algorithms to obtain the optimal path, and acquire the depth image.

The pseudo-code of procedure ComponentCut is as follows:

```
ComponentCut ( Component c, Threshold t)
{
        for each pixel p on c
        {
                d[8]← differences based on edge
                directions between p and its eight
                neighbor pixels (measured in angle
                between 0° to 360°)

                d_max←max(d[8])

                if d_max>=t then cut this pixel from
                c

        }
}
```

The edge direction of pixel p is computed using the Sobel filter. It is defined by

$$\mathrm{Dir}_{\mathrm{Sobel}}(p) = \arctan\left(\frac{G_v}{G_h}\right), \tag{1}$$

where G_v and G_h are the vertical and horizontal gradients, respectively, which are computed via convolution of p with Sobel filter kernels $\mathbf{C}_v$ and $\mathbf{C}_h$ defined by

$$\mathbf{C}_v = \begin{pmatrix} -1 & 0 & 1 \\ -2 & 0 & 2 \\ -1 & 0 & 1 \end{pmatrix}$$

and

$$\mathbf{C}_h = \begin{pmatrix} -1 & -2 & -1 \\ 0 & 0 & 0 \\ 1 & 2 & 1 \end{pmatrix},$$

respectively.

The matching value of pixel p in the left component image and pixel q in the right component image is computed using the modified normalized cross-correlation with a 5×5 window defined by

$$\mathrm{MatchingValue}(p,q) = \frac{\sum_{p_i\in A_p, q_j\in A_q}[(I_{p_i}-\bar{I}_p)*(I_{q_j}-\bar{I}_q)]}{\left[\sum_{p_i\in A_p}(I_{p_i}-\bar{I}_p)^2 * \sum_{q_j\in A_q}(I_{q_j}-\bar{I}_q)^2\right]^{1/2}}, \tag{2}$$

where A_p is a 5×5 window with center p, and A_q is a 5×5 window with center q; I_{p_i} and I_{q_j} are the corresponding pixel intensities of pixels p_i and q_j in the two windows A_p and A_q, respectively; and $\bar{I}_p$ and $\bar{I}_q$ are the average pixel intensities in the two windows A_p and A_q, respectively.

In the first step, the Canny edge detector is used to obtain edge images from the inputs. In the second step, component images are generated from the edge images. To generate component images from edge images, first an edge pixel is randomly selected as a component, namely, A. Then a new pixel is gradually added to component A if it is adjacent to a pixel in component A. A component is generated when no pixel can be added. The process is repeated until all edge pixels are visited.

Due to the natural difference of the left and right images, the detected edges in both edge images may not be consistent. As a result, the connected components in the two component images may not have a one-to-one relation. Usually, several components in the left component image are matched to one component in the right component image, and vice versa. Therefore, in the third step, to avoid this, the edges of each component in the left component image are cut by using procedure ComponentCut. Note that in the experiments, threshold t was set at 45 deg. In this step, asymmetric left and right component images are obtained. The relation of components in the asymmetric left and right component images is restricted to be many-to-one from the left to the right. Figure 3(a) shows real stereo input images "Church," Fig. 3(b) show component images, and Fig. 3(c) shows asymmetric component images. In Fig. 3(b), each color indicates one component. Matched components are shown in the same color in the left and right component images. Note that the Z-shaped component (pink red) in the left component image is matched to the 7-shaped component (pink red) in the right component image. Such matching is not desirable. In Fig. 3(c), after cutting the components in the left component image, the Z-shaped component is divided into the 7-shape component (light purple) and the

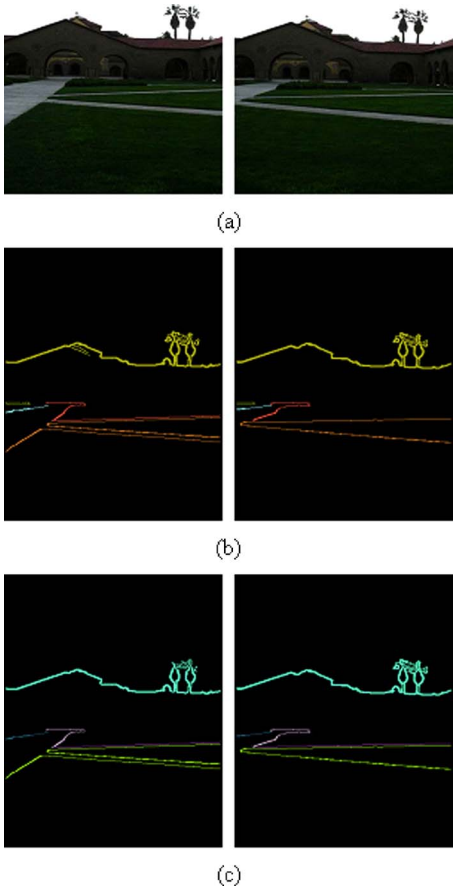

Fig. 3 (a) Real stereo input images "Church," (b) component images, and (c) asymmetric component images.

–shaped component (dark purple). Thus, this matching can be regarded as successful (7-shape (light purple) to 7-shape (light purple), –shaped (dark purple) to –shaped (dark purple)).

In the fourth step, the components between the asymmetric left and right component images are matched by introducing the concept of DSI by the components and applying DP techniques to find the optimal path of the DSI. "DSI by components" is defined as follows: element DSI$[i][j]$ of row r has no matching value if pixel p at coordinates (r,j) in the left component image is not an edge pixel or pixel q at coordinates *(r, j-i)* in the right component image is not an edge pixel. After applying the DP approach on this sparse DSI, every pixel in one component in the left component image is (or is not) matched to a pixel in one component in the right component image. A component has several pixels, and each of them may be matched to a particular component. The component matching process is done by counting the most matched components.

In the fifth step, the previous DSI is modified. The modification of DSI of row r is to cancel the matching value of element DSI$[i][j]$ if the component with pixel p at coordinates (r,j) is not matched to the component with pixel q at coordinates $(r,j-i)$. DP techniques are used to get the optimal path of the modified DSI and to obtain the matched pixel pairs of the matched component pairs. At this stage, the GCPs are generated.

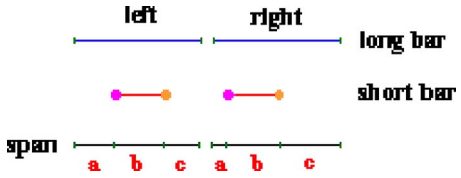

Fig. 4 Classification of two adjacent sides of a feature point of a GCP into a low-disparity side and a high-disparity side.

In the final step, after the GCPs are determined, they are put into the original DSI. The DSI is divided into several spans based on the GCPs. Spans here represent different objects or different parts of an object. The DP algorithms are applied piecewise in these spans. Figure 4 shows a vertical view of a scene consisting of two horizontal bars (the blue and red bars) for the left and the right eyes; the long bar is behind the short one. The GCPs here are represented as pairs of pink and orange points. The GCPs derive spans **a**, **b**, and **c** in the DSI. The two adjacent sides of a feature point of a GCP are classified into a low disparity side and a high disparity side. These GCPs clearly correspond to the foreground object (high disparity sides). The optimal paths on low disparity sides prefer low disparity paths by using different weights to adequately restrict the three directions in the DSI; the optimal paths on high disparity sides have to be attached to the GCPs. These weights are fixed to all inputs. In the experiments, the vertical matching weight was set at 30, the diagonal matching weight was set at 60, and the horizontal matching weight was set at 3. In addition, the points of the optimal paths in the spans of high disparity sides could not have larger disparities than one of the GCPs. This constraint is satisfied if the GCPs generated on the boundary of two objects represent the foreground object. Also, this condition is true when textures or colors of these two objects are not similar to that which is common for real scenes. This constraint implies that an upper bound of the disparities on the optimal path of the high disparity sides of the GCPs can be set.

4 Results

This section reports on the effectiveness of the proposed stereo matching algorithm.

Scharstein and Szeliski[17] compiled a good taxonomy of stereo matching algorithms and implemented most of them. Their programs can be downloaded from http://cat.middlebury.edu/stereo/code.html. They performed several experiments on stereo matching algorithms. Their experiments analyzed the effects of different building blocks on local and global stereo matching algorithms. In fact, the experiments are algorithms formed by combining or customizing various previous stereo matching algorithms. There are two kinds of parameters in the programs of Scharstein and Szeliski: independent of input data and dependent on input data. These parameters can be found in the script files bundled with their programs. The programs were used to generate depth maps for several stereo pairs. We just changed the parameters, which are dependent on

Table 1 Results of the test data

Stereo Image	Size	Time (s)	Max Disparity (pixels)
"Map"	568×216	1.3	29
"Tsukuba"	768×288	2.2	20
"Church"	640×480	13.6	60
"Classroom"	640×480	56.1	130
"Tower"	640×480	4.3	20

input data: the minimal disparity depth and the maximal disparity depth. A lot of results are generated for an input so the best two were chosen: one generated by a global algorithm and the other by a local algorithm. The generated depth maps were compared with the proposed approach. The platform used was a laptop with a Pentium M 1.5G CPU and 512 Mbytes of memory running the Microsoft® Windows XP Professional OS.

The experiment compared the present approach to the programs of Scharstein and Szeliski[17,21] using data of "Map," "Tsukuba," "Church," "Classroom," and "Tower," where "Map" and "Tsukuba" are synthesized stereo images; "Church," "Classroom," and "Tower" are real stereo images. Table 1 shows the experimental results. In this table, the names of experimental data are given in the first column, the second column shows the sizes of the experimental data, the computation time of the experimental data with the proposed algorithm are shown in the third column, and the last column shows the maximum disparities of the experimental data. The computation time is longer for "Church," much longer for "Classroom," and smaller for "Map," "Tsukuba," and "Tower". The maximum disparity is selected manually by roughly finding the disparity on the edge of nearest (to the view plane) objects. Also, this parameter is a user-supplied parameter in the programs of Scharstein and Szeliski.[17,21] In the experiments, the maximum disparity for "Map" was set at 29, for "Tsukuba" at 20, for "Church" at 60, for "Classroom" at 130, and for "Tower" at 20.

Figure 5(a) shows a stereo input pair "Map," Fig. 5(b) is a depth map generated by the proposed approach, Fig. 5(c) is a depth map generated by a global method with parameters set[17,21] as DPm1o20s0020, and Fig. 5(d) is a depth map generated by a local approach with parameters set[17,21] as SAD09bt10. For the depth maps of "Map," the proposed algorithm makes contours clearer than other conventional methods do. Figure 6(a) shows a stereo input pair "Tsukuba," Fig. 6(b) is a depth map generated by the proposed approach, Fig. 6(c) is a depth map generated by a global method with parameters set[17,21] as DPm1o20s0020, and Fig. 6(d) is a depth map generated by a local approach with parameters set[17,21] as SAD09bt20. The depth maps of "Tsukuba" generated by the proposed method and the conventional methods are almost the same. Figure 7(a) shows a real stereo input pair "Church," Fig. 7(b) is a depth map generated by the proposed approach, Fig. 7(c) is a depth map generated by a global method with parameters set[17,21] as DPm1o20s0020, and Fig. 7(d) is a depth map generated by a local approach with parameters set[17,21] as SAD09. Figure 8(a) shows a real stereo input pair "Classroom," Fig. 8(b) is a depth map generated by the proposed approach, Fig. 8(c) is a depth map generated by a global method with parameters set[17,21] as DPm1o20s0020, and Fig. 8(d) is a depth map generated by a local approach with parameters set[17,21] as SAD09. Figure 9(a) shows a real stereo input pair "Tower," Fig. 9(b) is a depth map generated by the proposed approach, Fig. 9(c) is a depth map generated by a global method with parameters set[17,21] as DPm1o20s0020, and Fig. 9(d) is a depth map generated by a local approach with parameters set[17,21] as SAD09. The depth maps of "Church," "Classroom," and "Tower" generated by the

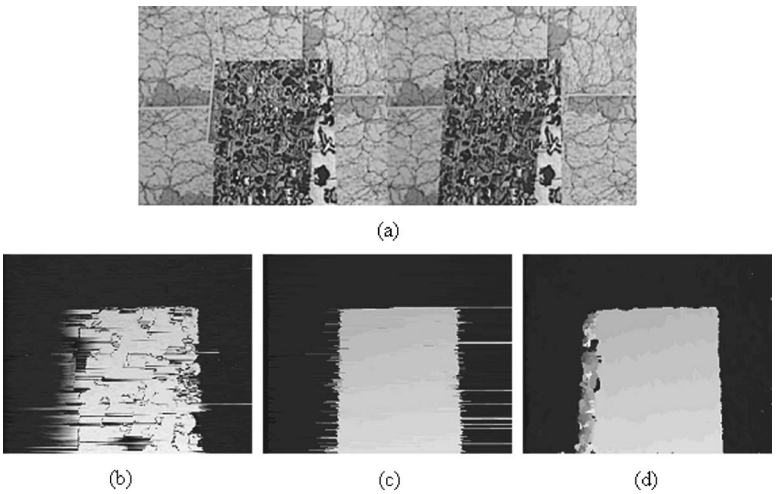

Fig. 5 (a) Stereo input pair "Map," (b) a depth map generated by the proposed approach, (c) a depth map generated by a global method with parameters set[17,21] as DPm1o20s0020, and (d) a depth map generated by a local approach with parameters set[17,21] as SAD09bt10; the maximum disparity set at 29.

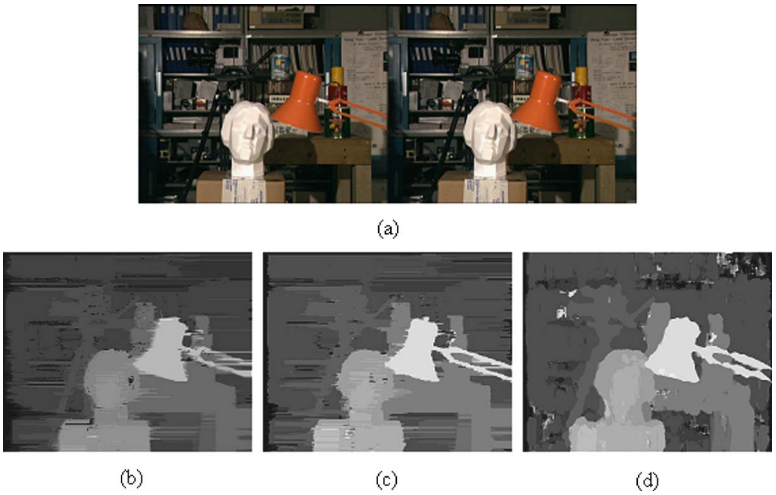

Fig. 6 (a) Stereo input pair Tsukuba, (b) a depth map generated by the proposed approach, (c) a depth map generated by a global method with parameters set[17,21] as DPm1o20s0020, and (d) a depth map generated by a local approach with parameters set[17,21] as SAD09bt20; the maximum disparity set at 20.

present method preserves the shapes of objects well. The algorithm also makes contours clearer than the conventional methods.

5 Analysis and Discussion

We proposed an asymmetric 2+1 pass approach for stereo matching to get a depth map from two real stereo images.

In the fourth step, the correctness of component matching is heavily influenced by edge detection. After the component matching is done, every component in the left component image is matched to one component in the right component image with hardly any exceptions. Thus, the GCPs (pixel p matching pixel q) must hold that pixels p and q are in the matched components.

For steps 4 and 5, both the component matching and the GCP generation are done with the DSI and the DP techniques. This has the advantage that the edges detected can be more than one unit wide or not even have an edge (they can be a region). That is, the proposed approach does not restrict GCPs to those edges that are only one unit wide. This could increase the possibility of finding right GCPs which would make the proposed approach reliable. Besides, it is efficient because of the sparseness of DSI.

For step 6, the GCPs could not simply be added onto the disparity image for doing the DP algorithms, although they are the trusted disparity pairs. Previous methods required only the optimal path on the DSI to pass through the GCPs. In the proposed algorithm, the obtained GCPs via the component matching only correspond to the high-disparity

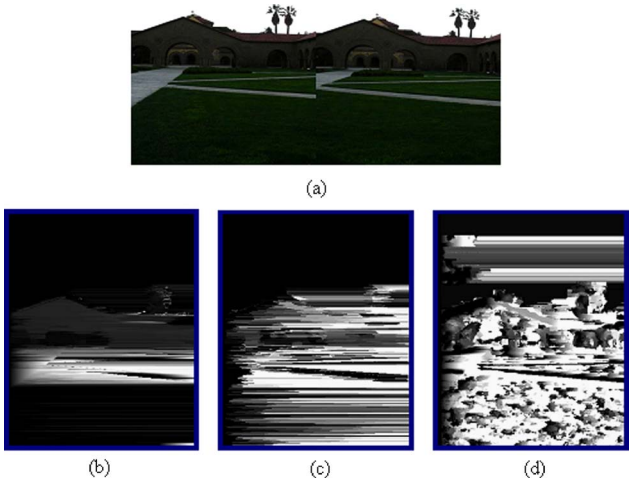

Fig. 7 (a) Real stereo input pair "Church," (b) a depth map generated by the proposed approach, (c) a depth map generated by a global method with parameters set[17,21] as DPm1o20s0020, and (d) a depth map generated by a local approach with parameters set[17,21] as SAD09; the maximum disparity set at 60.

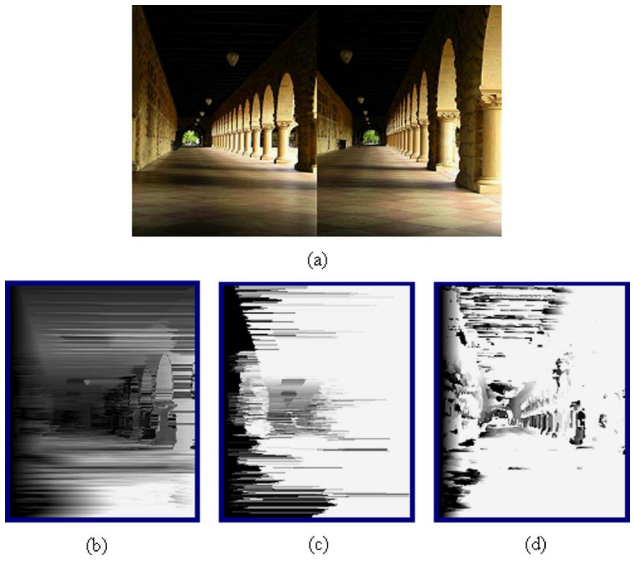

Fig. 8 (a) Real stereo input pair "Classroom," (b) a depth map generated by the proposed approach, (c) a depth map generated by a global method with parameters set[17,21] as DPm1o20s0020, and (d) a depth map generated by a local approach with parameters set[17,21] as SAD09; the maximum disparity set at 130.

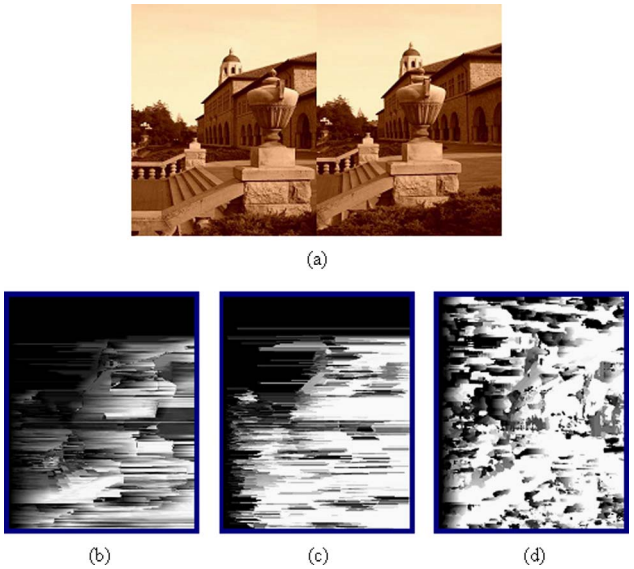

Fig. 9 (a) Real stereo input pair "Tower," (b) a depth map generated by the proposed approach, (c) a depth map generated by a global method with parameters set[17,21] as DPm1o20s0020, and (d) a depth map generated by a local approach with parameters set[17,21] as SAD09; the maximum disparity set at 20.

sides. In fact, the obtained GCPs via the component matching correspond only to the high-disparity sides of its two adjacent surfaces. Thus, the adjacent sides of the GCPs are classified into low-disparity sides and high-disparity sides. Also, applying the DP approach piecewise is logical. Because the generated GCPs are most likely to be on the object edges, the spans in the DSI derived by the GCPs represent different objects or different parts of an object, and therefore, their depths should be different. Because the GCPs have large disparities (detected edges belong to the front object), the points of the optimal path in the spans of high disparity sides have to be restricted so that they do not have larger disparities than the GCPs.

Although the DP algorithms are used three times, the computation time only depends on the "Max Disparity" chosen when making the DSI. Therefore, if the maximum disparity between the stereo images is smaller, less computation time will be needed.

6 Conclusions

An asymmetric 2+1 pass algorithm was presented for stereo matching to generate a depth map from the input of two real stereo images. The main contributions of the proposed method are as follows: (1) a method for cutting the edges of each component in the left component image is proposed to obtain asymmetric left and right component images for improving matching; (2) the proposed approach produces reliable and efficient matching for the real stereo images; (3) the proposed algorithm has the advantage that the edges detected can be more than one unit wide or not even have an edge (they can be a region), this would make the proposed approach reliable, besides, it is efficient because of the sparseness of DSI, and (4) the algorithm preserves the shapes of objects well and it makes contours clearer than the other methods.

Even though the quality of the depth maps from the real stereo images has been improved, there still are some errors, especially in the smooth areas. Because the edge detection is not perfect, not all the GCPs can be determined. Another problem is that the depth map made with the DP algorithms is striated. These problems will be addressed in future research.

Acknowledgments

This research was partially supported by the National Science Council under grant NSC 94-2213-E-239-009.

References

1. F. Bobick and S. S. Intille, "Large occlusion stereo," *Int. J. Comput. Vis.* **33**(3), 181–200 (1999).
2. R. C. Bolles, H. H. Baker, and M. J. Hannah, "The JISCT stereo evaluation," in *Proc. DARPA Image Understanding Workshop*, pp. 263–274 (1993).
3. J. Cox, S. Hingorani, and S. Rao, "A maximum likelihood stereo algorithm," *Comput. Vis. Image Underst.* **63**(3), 542–567 (1996).
4. J. Cryer, P. S. Tsai, and M. Shah, "Integration of shape from x modules: combining stereo and shading," in *Proc. 1993 IEEE Computer Society Conf. on Computer Vision and Pattern Recognition CVPR*, pp. 15–17 (1993).
5. M. Gong and Y. H. Yang, "Genetic-based stereo algorithm and disparity map evaluation," *Int. J. Comput. Vis.*, **47**(1–3), 63–77 (2002).
6. M. Gong and Y. H. Yang, "Fast stereo matching using reliability-based dynamic programming and consistency constraints," in *Proc. 9th IEEE Int. Conf. Computer Vision (ICCV)*, pp. 610–617 (2003).
7. M. J. Hannah, "Computer matching of areas in stereo images," PhD. Thesis, Stanford University (1974).
8. L. Hong and G. Chen, "Segment-based stereo matching using graph cuts," in *Proc. 2004 IEEE Computer Society Conf. on Computer Vision and Pattern Recognition 2004 (CVPR 2004)*, Vol. **1**, pp. I-74–I-81 (2004).
9. A. Ignatenko and A. Konushin, "A framework for depth image-based modeling and rendering," in *Proc. 13th Int. Conf. on Computer Graphics and Vision GraphiCon-2003*, pp. 169–172 (2003).
10. H. Jeong and S. C. Park, "Trellis-based systolic multi-layer stereo matching," in *Proc. IEEE Workshop on Signal Processing Systems*, pp. 257–262 (2003).
11. S. B. Kang, R. Szeliski, and J. Chai, "Handling occlusions in dense multi-view stereo," in *Proc. 2001 IEEE Computer Society Conf. on Computer Vision and Pattern Recognition (CVPR)*, Vol. **1**, pp. I-103–I-110 (2001).
12. K. M. Lee and C. C. J. Kuo, "Shape reconstruction from photometric stereo," in *Proc. 1992 IEEE Computer Society Conf. on Computer Vision and Pattern Recognition (CVPR)*, pp. 479–484 (1992).
13. M. H. Lin and C. Tomasi, "Surfaces with occlusions from layered stereo," in *Proc. Conf. on Computer Vision and Pattern Recognition* (2003).
14. M. G. Mostafa, S. M. Yamany, and A. A. Farag, "Integrating stereo and shape from shading," in Proc. 1999 Int. Conf. on Image Processing (ICIP), pp. 130–134(1999).
15. Y. Ohta and T. Kanade, "Stereo by intra- and inter-scanline search using dynamic programming," *IEEE Trans. Pattern Anal. Mach. Intell.*, **7**, 139–154 (1985).
16. R. Sara, "Finding the largest unambiguous component of stereo matching," in *Proc. 7th Eur. Conf. on Computer Vision (ECCV)*, pp. 900–914 (2002).
17. D. Scharstein and R. Szeliski, "A taxonomy and evaluation of dense two-frame stereo correspondence algorithms," *Int. J. Comput. Vis.*, **47**(1–3), 7–42 (2002).
18. J. Sun, N. N. Zheng, and H. Y. Shum, "Stereo matching using belief propagation," *IEEE Trans. Pattern Anal. Mach. Intell.* **25**(7), 787–800 (2003).
19. P. H. S. Torr and A. Criminisi, "Dense stereo using pivoted dynamic programming image," *Image Vis. Comput.* **22**, 795-806 (2004).
20. C. L. Zitnick and T. Kanade, "A cooperative algorithm for stereo matching and occlusion detection," *IEEE Trans. Pattern Anal. Mach. Intell.* **22**(7), 675–684 (2000).
21. http://cat.middlebury.edu/stereo/code.html.
22. J. Canny, "A computational approach to edge detection," *IEEE Trans. Pattern Anal. Mach. Intell.* **8**(6), 679–698 (1986).

Chi Chu received his BS degree in applied mathematics and his MS degree in computer and information science in 2003 and 2005, respectively, from National Chiao Tung University in Hsinchu, Taiwan, where he is currently a PhD student in the Department of Computer Science. His current research interests include computer graphics, especially artistic rendering and computer animation.

Chin-Chen Chang received his PhD degree in computer and information science from National Chiao Tung University in Hsinchu, Taiwan, in 1998. He is currently an assistant professor with the Department of Computer Science and Information Engineering, National United University in Miaoli, Taiwan. His current research interests include image-based rendering, computer graphics, and human-computer interface.